

# Optical Binding in Air

M. Guillon

Laboratoire d'Interférométrie Stellaire et Exoplanétaire, France

**Abstract**—Optical binding between micron-sized oil droplets in air has recently been observed. The experimental setup, consisting in two vertical, counter propagating and diverging laser beams, builds up a three dimensional trap. The cloud of oil droplets, enclosed in a glass cell, progressively fills in the trap where droplets interact one with another. Scattered intensity is observed on a video camera. Interactions involve optical, electrostatic, radiometric and capillary forces. Orders of magnitude are discussed.

Chains up to four droplets have been observed, the most stable structure being the doublet and not the single drop. In air, viscosity being one thousand times smaller than in water, mean free path of a micro-sphere is much bigger. That is why mean residence times in metastable states are of the magnitude of a few seconds and that brownian motion quickly drives the trapped droplets in the very minimum of potential energy: the doublet structure. Two stable states have also been obtained for the doublet. Observation of interference indicates that oil droplets are phase-locked onto each other every  $\lambda/2$ .

The spraying technique we use, gives droplets smaller than the micron in radius. This is the intermediate case of the Mie range between the small and large wavelength cases. Those new experimental results exhibit the role of the short and long range interactions in optical binding. They are then theoretically discussed both in the ray model and in the Rayleigh approximation, and compared with previous works on optical binding in water. Moreover, in our case, the index contrast is much bigger. It implies stronger scattered intensities, bigger interaction forces with light and therefore, bigger binding forces.

## 1. Introduction

Since the pioneering work by Ashkin [1] in the early 1970's, optical tweezers have nowadays become a commonly used tool for micromanipulation in water. Optical trapping in air and vacuum remains a difficult task due to Van der Waals forces several orders of magnitude larger than optical forces. In the literature, two possibilities were explored: the use of aerosols [1–4] and mechanical vibration coupled with strongly focused cw laser beams [5, 16, 7, 8]. Afterwards, self-assembled structures of microparticles under strong laser illumination have been demonstrated [9–12]. Optical binding was observed when the particle separation is either orthogonal or along the light propagation. When the separation is set orthogonal to the beam propagation and to beam polarization, theory predicts potential minima every  $\lambda$  for particles in the Rayleigh range [13]. This  $\lambda$  periodicity was experimentally observed for polystyrene spheres in the Mie range in water [10]. The Mie correction to Rayleigh approximation was supposed to modify the interaction strength more than the periodicity. In three dimensional optical traps made with two counter-propagating beams, potential minima appeared to be along the beam axis. Due to the weakly focused beams and to gradient forces, the particles are constrained to remain on the beam axis. Optical interactions then lead to chains where spheres are either stuck or separated by more than a diameter away [12]. For spheres in the Rayleigh range, potential minima every  $\lambda/2$  are expected.

Trapping in air imposes a tridimensional trap since the Van der Waals forces are not negligible as is the case in water. However, the larger index ratio gives larger cross sections and the optical forces are consequently stronger than in water.

## 2. Experiment

Our experiment [15] deals with micron-sized oil-droplets in air obtained with a spray nozzle. According to their falling time, their diameter was estimated to be in the range between  $1\ \mu\text{m}$  and  $1.5\ \mu\text{m}$ . They are protected from air convection currents by a glass cell. We use a 30 mW frequency doubled YAG laser at 532 nm. The optical trap consists in two weakly focused ( $N.A. = 1/15$ ) and counter-propagating laser beams (see Fig. 1). The return beam is focused roughly  $300\ \mu\text{m}$  before the forward beam. The equilibrium position of trapped particles is at half distance of both focusing points, where the intensities of the two beams are equal. The geometry is then similar to those previously studied in water [11, 12] with optical fibers. We chose a vertical geometry in order to oppose gravity with the scattering force rather than with the gradient force which is much weaker for spheres in the Mie range.

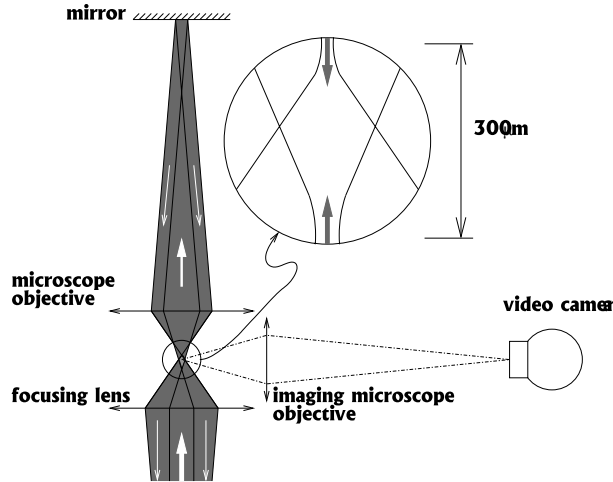


Figure 1: Experiment principle. The scattering force is opposed to gravity. The forward beam is retro-reflected on a mirror at the focus of a lens. The downward returning beam is focused  $300\ \mu\text{m}$  above the upward direct beam so as to build a stable equilibrium zone. The laterally scattered intensity is observed on a video camera through a 10x, 0.25NA microscope lens. A cell of glass, not shown, protects from air motion.

### 3. Results

#### 3.1. Trapped Structures

When the cell is filled with an oil droplet cloud, radiation pressure pushes the droplets inside the trap. By far, the most common structure observed was a doublet. We rarely saw a single droplet. Three and four droplet chains were also seen for a few seconds before changing into a doublet by escaping or merging processes. Coalescence with outer droplets—tends to increase progressively the size of both droplets in a doublet. The increasing finishes when the cloud of droplet has fallen down. We observed that in a doublet, the larger the droplets, the further apart. We never saw a doublet collapsing or splitting away. The optical binding forces in this case, appears to be much stronger than all other forces.

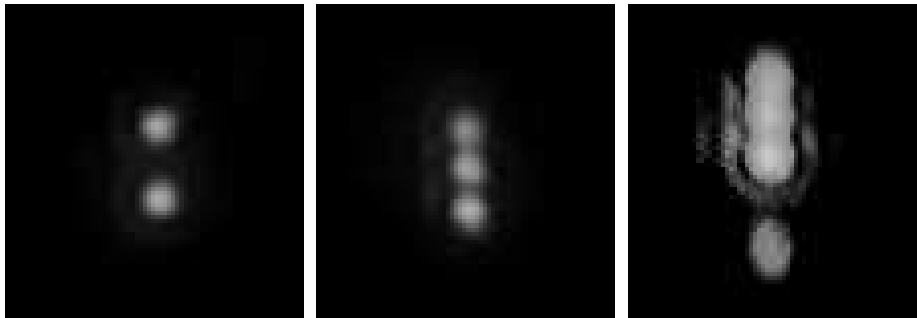


Figure 2: Doublet, triplet and quadruplet structures. The doublet is observed to be the most stable structure is the doublet. Its droplets are spaced approximately  $3.5\ \mu\text{m}$  apart, between centers. The length scale is the same for all the pictures.

On a few occasions, we observed a sudden change of the doublet's appearance, mainly regarding the interference of both Airy patterns on the camera. On the first picture (see Fig. 3), images of droplets interfere such as to give a dark fringe between droplets while on the second picture, we see bright dots on the symmetry axis. In the first case, droplets are scattering in phase opposition as in the second case, they are emitting in phase, corresponding to a  $\lambda/2$  difference of distance. An estimate of the difference of distance separations of doublets gave values close to  $\lambda/2$ . This measurement is difficult due to the low resolution power of the imaging microscope objective. This phenomenon was assumed to be a switching between two stable states of a doublet, which can be understood in the dipolar approximation as explained further.



Figure 3: Two different equilibrium states of a  $2.3\ \mu\text{m}$  doublet. The main difference is the interference pattern. On the first picture, droplets are emitting in phase opposition, we see a dark fringe on the symmetry axis. On the second one, they are emitting in phase, bright dots can be seen on the symmetry axis. It suggests that the difference of separation distance between droplets increased. We estimated the increasing to be of the order of half a wavelength in accordance with the interference pattern.

### 3.2. Clinging to Fringes

When trapped, particles move quickly due to speckle. Static speckle is introduced with dirtiness of optical components. Dynamic speckle is also introduced by the cloud of droplets crossing the trapping beams. Disturbance caused by the cloud is larger when a droplet cross the beam in the vicinity of the focusing point.

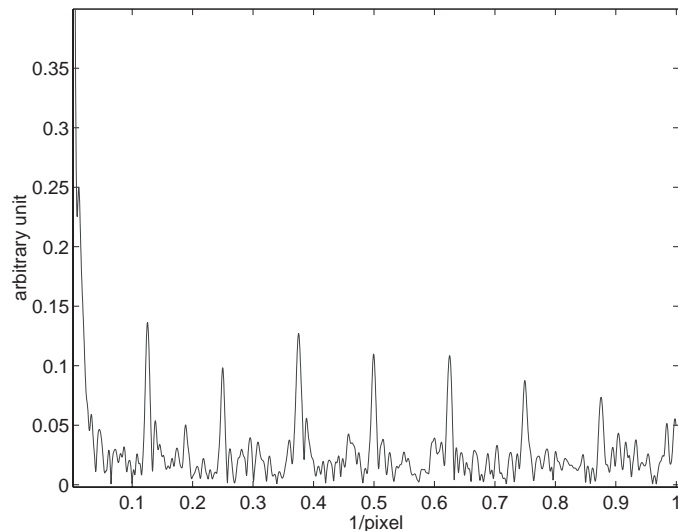


Figure 4: Position spectrum of the doublet in the trap.

The laser we use has two longitudinal modes. There are coherence beatings every three millimeters. After a 30 cm optical path, we do not know if the return beam is coherent with the upward one. In the case where the two counter-propagating beams are coherent, a stable  $\lambda/2$  fringe pattern should trap the structure. If the brightness contrast is not large enough, the gradient force is weak and small intensity fluctuations between the two counter propagating beams can unbalance the well's minimum in the longitudinal direction. In this case, the doublet quickly (compared with the frame rate of the video camera) sweeps a sinusoidal potential well. As images of droplets are several pixels wide, their positions can be measured with a subpixel resolution. We performed the Fourier transform of the positions  $y_p$  of the doublet in the trap when counter-propagating beams were circularly polarized and weakly coherent (see Fig. 4):

$$\mathcal{F}(Y)(\sigma) = \sum_p e^{2\pi i \sigma y_p}$$

The same numerical calculation for the case of a crossed-polarized beams experiment does not give those peaks. According to imaging power  $\lambda/2 \simeq 1.6\ \text{pixel}$ , the main harmonic is then the 0.62 peak. The other peaks are folded back harmonics. We can see that they are numerous and Dirac comb like, which means that the doublet very likely mechanically clings to fringes and the position spectrum we obtain cannot be a light modulation measurement artefact.

### 3.3. Theoretical Discussion on Binding

In our experiment, the spheres radii are from  $0.5 \mu\text{m}$  up to  $1.2 \mu\text{m}$  when several droplets have merged. Those values correspond to  $ka$  ( $a$  being its radius and  $k$  the wave vector) between 12 and 14. For particles in the Mie regime which is the case, numerical calculations have to be performed and multiscattering processes must be taken into account to know the exact optical binding forces [14]. However, in this regime, the particles' behaviour looks like both dipoles and large spheres. In this discussion, we aim at giving a flavour of the physics of the binding effect. We think this experiment can be approximately understood from the two extreme regimes of the ray model and the Rayleigh range.

When spheres are such that  $ka < 1$  or when  $kr > 1$  ( $r$  being the separation distance between spheres), the dipole approximation is sufficient to estimate potential minima. In this approximation, optical interactions between particles are maximal when the separation is orthogonal to polarization. It can be either along or transverse to the beam axis. In agreement with dipolar theory, it was experimentally observed [10] that potential wells for two particles were every  $\lambda$ , the wavelength. When the separation is along the wave vector, a similar calculation predicts potential wells roughly every  $\lambda/2$ :

$$V = - \left| \frac{\cos \varphi + f(kr)e^{ikr} \cos(kr + \varphi)}{1 - f(kr)^2 e^{2ikr}} \right|^2$$

with

$$f(kr) = k^3 \alpha \left( \frac{1}{kr} - \frac{1}{(kr)^3} + \frac{i}{(kr)^2} \right)$$

$\alpha = \frac{n^2 - 1}{n^2 + 2} a^3$  being the polarizability of the (identical) dielectric spheres of index  $n$ , and  $r$  being the separation between the two spheres. The denominator corresponds to the Mossotti resonance in atom trapping. It can only be zero for resonant particles for which the real part of  $f$  can be larger than one. This can never happen with dielectric or even metallic particles: the spheres touch before the resonance happens. When  $kr > 1$ , we can approximate the previous formula by:

$$V \simeq - \cos \varphi \left( \cos \varphi \left( 1 + \frac{k^3 \alpha}{kr} \right) + \frac{k^3 \alpha}{kr} \cos(2kr + \varphi) \right)$$

which exhibit a  $\lambda/2$  periodicity which is consistent with the experimental observation (Fig. 3).

However we could not see jumps between many  $\lambda/2$ -separated potential wells like in Fournier's experiment [10]. The two droplets remain at a quite stable distance depending on their size. This comportement looks like that of large spheres.

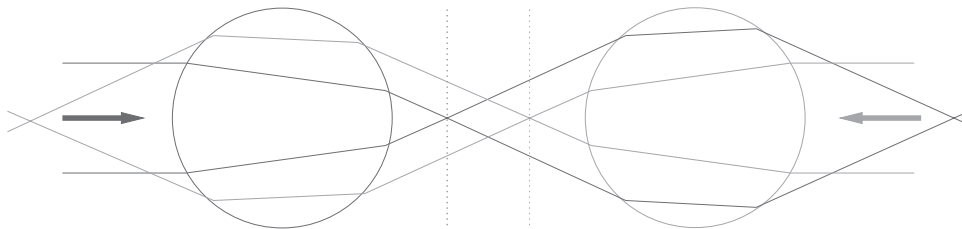


Figure 5: Principle of binding between two spheres in the ray model. Each droplet acts as a tweezer for the other. As there is no reason why focal plans of spheres be the same, the second sphere defocuses its trapping tweezer and can rebuild another tweezer behind it like in triplet cases or 4-droplet cases.

When the radius of spheres is such that  $ka > 100$ , optical forces can be calculated in the ray model approximation with a good degree of accuracy [6, 17]. In this model, binding between two spherical dielectric particles can be understood by comparison with optical tweezers. For a sufficiently focused beam, a dielectric particle can be trapped close to the focal point. In our case, the focusing lens is nothing else than the next droplet. Each droplet builds an optical tweezer for the other. The numerical aperture of a spherical lens can be approximated by  $NA \simeq \frac{a}{f} = 2 \frac{n-1}{n}$  which only depends on the index of the sphere (not on its radius). We think this model explains the high stability of the doublet structure despite speckle: a single plane seems to be sufficient for particles to be bound. For reaching such stability, spheres need to be close enough to each other.

When spheres are much more than a diameter away like in the case of experiments in water [11, 12], spheres cannot be in a bound state: the focusing numerical aperture is not sufficient for the optical tweezer to be stable. In this case, microspheres interact repulsively in a single trap so as to give chains. This comparison with optical tweezers can also explain why structures with three and four droplets are less stable than the doublet case. Indeed, while being trapped by the tweezer, the sphere defocuses the beam (see Fig. 5). However, there is no reason why the optical force be zero when the focal point of the first droplet is the same as the focal point of the second. We can then hope, for a given radius of sphere (even more in the Mie range) a configuration where the second sphere will be trapped at two focal lengths of the focusing point. In this case, neglecting spherical aberrations, the second sphere will rebuild a trap behind it. This argument explains both the possibility to build 4-droplet chains and why the doublet is much more stable than triplets and quadruplets.

### 3.4. Orders of Magnitude

We can see on movies than despite all the disturbing sources, the doublet is very stable, even when the laser beam is cut for one second. We present here the main forces involved in this experiment.

The strongest forces are capillary forces. For particles smaller than  $1.2 \mu\text{m}$  in radius, they can be estimated with Laplace's theorem:  $\Delta P = \frac{2\gamma}{a} \simeq 10^5 \text{ pN} \cdot \mu\text{m}^{-2}$  where  $\Delta P$  is the pressure difference between inside and outside the droplet,  $\gamma$  is the capillary coefficient of the liquid and  $a$  the radius of the sphere. This pressure must be compared with the electromagnetic pressure of the order of  $I/c$ . In a binding case, field can be enhanced between particles so as to increase the optical force by one order of magnitude. However, if we simply consider the trapping pressure, we obtain in the case of our experiment a pressure equal to  $1 \text{ pN} \cdot \mu\text{m}^{-2}$ .

Brownian motion could also destruct the phase locking observed between bound droplets. As the interference pattern between images of droplets of a doublet remains despite random forces, we can conclude that the distance never changes more than  $\lambda/4$ . It means that the mean thermal force over a distance  $\lambda/4$  is smaller than  $\frac{kT}{\lambda/4} \simeq 10^{-2} \text{ pN}$ . To be compared with the pressures we calculated in the previous paragraph, we can approximate the radius of spheres to be one micron. Finally, as droplets are negatively charged when sprayed due to triboelectricity effects with the spray nozzle, electrostatic forces causes droplet repealing. Each droplet carry a few elementary charges and the distance between droplets being roughly  $2.5 \mu\text{m}$ :  $F = \frac{1}{4\pi\epsilon_0} \frac{qq'}{r^2} \simeq 10^{-5} \text{ pN}$ . Electrostatic forces are then three orders of magnitude smaller than optical forces.

We should add an estimate of heating effects. As oil slightly absorbs light, convection currents may appear inside droplets. This effect has already been discussed in a previous article [15] but a precise idea of the forces involved cannot be given.

## 4. Conclusion

Our experimental results obtained in air differ appreciably from those previously reported in water. Much of the difference probably results from the higher index contrast. Our results fit both with a Rayleigh range binding process and a semi-classical ray model.

## Acknowledgment

I would like to thank particularly Professor A. Labeyrie for fruitful advice and support, and acknowledge Professor J.-M. Fournier for his helpful encouragement.

## REFERENCES

1. Ashkin, A., *Phys. Rev. Lett.*, Vol. 24, 156–159, 1970.
2. Ashkin, A. and J. M. Dziedzic, *Appl. Phys. Lett.*, Vol. 28, No. 6, 333–335, 1975.
3. Magome, N., M. I. Kohira, E. Hayata, S. Mukai, and K. Yoshikawa, *J. Phys. Chem. B*, Vol. 107, 3988–3990, 2003.
4. Hopkins, R. J., L. Mitchem, A. D. Ward, and J. P. Reid, *Phys. Chem. Chem. Phys.*, Vol. 6, 4924–4927, 2004.
5. Ashkin, A. and J. M. Dziedzic, *Appl. Phys. Lett.*, Vol. 19, No. 8, 283–285, 1971.
6. Pocholle, J.-P., J. Raffy, Y. Combemale, M. Papuchon, G. Roosen, and M. T. Plantegenest, *Appl. Phys. Lett.*, Vol. 45, No. 4, 350–352, 1984.
7. Omori, R., T. Kobayashi, and A. Suzuki, *Opt. Lett.*, Vol. 22, No. 11, 816–818, 1997.

8. Omori, R., K. Shima, and A. Suzuki, *Jpn. J. Appl. Phys.*, Vol. 38, L743–L745, 1999.
9. Burns, M., J.-M. Fournier, and J. A. Golovchenko, *Science*, Vol. 249, 749–754, 1990.
10. Burns, M., J.-M. Fournier, and J. A. Golovchenko, *Phys. Rev. Lett.*, Vol. 63, No. 12, 1233–1236, 1989.
11. Tatarkova, S. A., A. E. Carruthers, and K. Dholakia, *Phys. Rev. Lett.*, Vol. 89, 283901,1–4, 2002.
12. Singer, W., M. Frick, S. Bernet, and M. Ritsch-Marte, *J. Opt. Soc. Am. B*, Vol. 20, No. 7, 1568–1574, 2003.
13. Depasse, F. and J.-M. Vigoureux, *J. Phys. D: Appl. Phys.*, Vol. 27, 914–919, 1993.
14. Moine, O. and B. Stout, *J. Opt. Soc. Am. B*, Vol. 22, 8, 2005.
15. Guillon, M., *SPIE Proceedings*, 5930–62, 2005.
16. Roosen, G., *C. Imbert, Phys. Lett.*, Vol. 59A, 6, 1976.
17. Gussgard, R., T. Lindmo, and I. Brevik, *J. Opt. Soc. Am.* Vol. B, No. 9, 10, 1991.